Science of the Total Environment 823 (2022) 153693

Contents lists available at ScienceDirect

Science of the Total Environment

journal homepage: www.elsevier.com/locate/scitotenv

# Valorization of UWWTP effluents for ammonium recovery and MC elimination by advanced AOPs

Dennis Deemter [a], Irene Salmerón [a], Isabel Oller [a], Ana M. Amat [b], Sixto Malato [a,*]

[a] Plataforma Solar de Almería-CIEMAT, Carretera de Senés Km 4, Tabernas, Almería, Spain
[b] Grupo Procesos de Oxidación Avanzada, Campus de Alcoy, Universitat Politècnica de València, Spain

## HIGHLIGHTS

- Ammonium was successfully recovered from wastewaters with nanofiltration.
- Solar assisted anodic oxidation was the most effective treatment.
- Permeates from concentration factor > 2 were non-suitable for direct irrigation.

## GRAPHICAL ABSTRACT

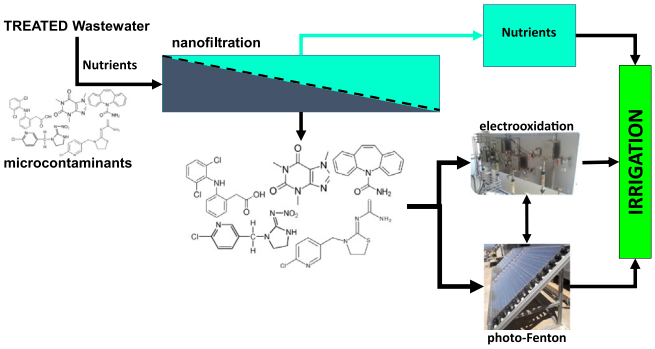


## ARTICLE INFO

*Article history:*
Received 5 November 2021
Received in revised form 10 January 2022
Accepted 1 February 2022
Available online 6 February 2022

Editor: Dimitra A Lambropoulou

*Keywords:*
Contaminants of emerging concern
Nanofiltration retentate
Solar advanced oxidation processes
Tertiary treatment
Urban wastewater reuse

## ABSTRACT

The main objective of this study was to generate ready-to-use revalorized irrigation water for fertilization from urban wastewater treatment plant (UWWTP) effluents. The focus was on controlled retention of $NH_4^+$ and microcontaminants (MC), using nanofiltration. Retentates generated were treated by solar photo-Fenton at circumneutral pH using Ethylenediamine-N, N′-disuccinic acid (EDDS) iron complexing agent. Solar photo-Fenton degradation efficacy was compared with electrooxidation processes as anodic oxidation, solar-assisted anodic oxidation, electro-Fenton and solar photoelectro Fenton. Finally, phytotoxicity and acute toxicity tests were performed to demonstrate the potentially safe reuse of treated wastewater for crop irrigation. Nanofiltration was able to produce a ready-to-use permeate stream containing recovered $NH_4^+$. (valuable nutrient). Solar photo-Fenton treatment at circumneutral pH would only be of interest for rapid degradation of contaminants at less than 1 mg/L in nanofiltration retentates. Other alternative tertiary treatments, such as electrooxidation processes, are a promising alternative when a high concentration of MC requires longer process times. Anodic oxidation was demonstrated to be able to eliminate >80% of microcontaminants and solar-assisted anodic oxidation significantly reduced the electricity consumption. Electro-Fenton processes were the least efficient of the processes tested. Phytotoxicity results showed that irrigation with the permeates reduced germination, root development was mainly promoted and shoot development was positive only at low retention rate (concentration factor = 2). Acute and chronic *Daphnia magna* toxicity studies demonstrated that the permeate volumes should be diluted at least 50% before direct reuse for crop irrigation.

## 1. Introduction

The production of synthetized fertilizers is a large global consumer of energy. Life is already endangered by the need for new farmlands due to soil erosion and saturation, by the inappropriate and excessive use of fertilizers and salination by unsuitable irrigation sources (Fernández-Delgado

* Corresponding author.
*E-mail address:* sixto.malato@psa.es (S. Malato).

http://dx.doi.org/10.1016/j.scitotenv.2022.153693

et al., 2020). It is therefore of paramount importance to find alternative ways to produce these fertilizers. Novel processes are already being explored to minimize energy demand on fertilizers production and overall environmental impact. A good example are solar fertilizers (to replace the centralized, fossil-fuel based Haber-Bosch process with a distributed network of modules that would use solar power to pull nitrogen from the atmosphere and also to catalyze the splitting of water molecules to get hydrogen), which aim at alternative, decentralized production of fertilizers with renewable solar energy (Comer et al., 2019; Hargreaves et al., 2020). Another promising way of recovering nutrients for fertilizers comes directly from urine, as it contains the primary macro nutrients: nitrogen, phosphorus and potassium. However, urine collection and effective nutrient recovery are challenging, as single systems are not yet sufficient, and combination and integration of existing systems are still in its early states (Gerardo et al., 2015; Patel et al., 2020; Wei et al., 2018).

The recovery of ammonium from agricultural, industrial, and urban wastewater (UWW) has also a strong potential for reducing the energy necessary to produce synthetized fertilizers, as the streams coming from these sources are generally easy to isolate, highly concentrated or already connected to existing infrastructures (Sakar et al., 2019). In agriculture, this could contribute to treatment of neighboring or nearby surface water bodies using recovery technologies to prevent excessive algae growth or sudden death of microorganisms, and prevent early soil saturation by fertilizers, salts, heavy metals and other contaminants. Thus, reducing pollution and delivering a renewable, sustainable source of revalorized irrigation water would make a synergetic contribution to synthetized fertilizer production, by lowering both the overall economic and environmental footprint (Zeng et al., 2020).

Although the high potential for ammonium recovery from UWW is widely known, such wastewater also contains traces and even high concentrations of pollutants, and therefore, it must be sanitized before its reclamation. Microcontaminants (MCs) in wastewater, known as Contaminants of Emerging Concern (CECs), are in the range of ng/L to μg/L (van Gils et al., 2020). They come from the consumption and disposal of everyday products, such as cosmetics, pesticides, pharmaceuticals and other organic compounds, which are either incorrectly disposed of, or simply cannot be treated by conventional wastewater treatment methods (Farré, 2020; Seibert et al., 2020; Taylor et al., 2020). The resulting bioaccumulation, endocrine disruption, chronic toxicity, irreversible soil pollution and saturation are of “emerging concern”, and demand rapid attention by the combination and/or reinforcement of conventional treatment methods with new technologies (Balogun et al., 2019; Yusuf et al., 2020).

The use of nanofiltration (NF) membranes can be considered an interesting option for tackling the problem of low removal rate of MCs in conventional wastewater treatments. Other membranes of higher pore size (as microfiltration) do not retain MCs. NF is relatively simple and inexpensive, and it could lower treatment costs by (pre)concentrating MCs and reducing the total volume of contaminated streams to be treated, with the subsequent reduction of reagents requirement and plant size (Miralles-Cuevas et al., 2017). Furthermore, NF does not retain ammonium and other needed inorganics, the operation and maintenance costs are lower than reverse osmosis, while organic MC rejection rates remain high (Mendret et al., 2019). The two main types, according to the membrane material, of NF membranes are the cheaper polymeric and the more expensive ceramic membranes. NF membrane selectivity depends on a variety of parameters, which determine the main physicochemical separation mechanisms of size exclusion, solution-diffusion and Donnan effect, such as the molecular and surface charge, concentration, pH, pore size and morphology. Furthermore, system parameters, such as flow rate, pressure and temperature affect process control and optimization (Schäfer and Fane, 2021; Wang and Lin, 2021; Wang et al., 2021). Understanding these mechanisms and parameters for revalorization of wastewater streams is a clear objective of the scientific community (Castro-Muñoz and Fíla, 2018; Nath et al., 2018; Suwaileh et al., 2020). In addition, the promising solutions offered by membrane technologies for recovering nutrients, such as ammonium, have recently been gaining attention, especially in remote and emerging areas, where infrastructures are commonly absent or deficient and fossil fuels are required to transport the nutrients. Recovered nutrients can also dramatically boost agricultural yields, contributing to health and economic development (Chen et al., 2020).

Although NF rejection rates are high and can produce the desired high-quality permeate streams for direct applications, rejection of MCs strongly depends on the abovementioned parameters and varies for every specific compound (Xu et al., 2020). This dependency requires its combination with advanced treatment technologies to prevent MCs being left in the membrane concentrate, which requires further treatment. The most recently studied advanced treatments that offer this versatility are advanced oxidation processes (AOPs).

AOPs generate highly reactive nonselective hydroxyl radicals ($HO^{\bullet}$), which can be deployed for the elimination of MCs. One of these, photo-Fenton, is based on iron catalysis ($Fe^{2+}/Fe^{3+}$) under UV–vis light and hydrogen peroxide ($H_2O_2$). The process uses simple chemicals and can be powered by renewable solar radiation using solar compound parabolic collectors (CPC) (Horikoshi and Serpone, 2020; Malato et al., 2009).

Although classic photo-Fenton must be applied at acidic pH to avoid iron precipitation, iron complexing agents, now under study, can maintain iron in solution at circumneutral pH. Ethylenediamine-N, N′-disuccinic acid (EDDS), for example, has shown successful application at pH 6, and even up to pH 9 (Wang et al., 2019). EDDS is biodegradable, and therefore environmentally-friendly (López-Rayo et al., 2019; Temara et al., 2006).

Combinations of different oxidation methods are also currently being promoted to increase MC elimination efficiency. Electrochemical processes, for instance, combine nicely with the Fenton reaction, since they can simultaneously generate different oxidizing agents on the anode surface (mainly $HO^{\bullet}$, $ClO^{-}$ and $SO_4^{\bullet-}$) depending on the ionic composition of the (UWW) effluent and the nature of the anode (Salmerón et al., 2021). $H_2O_2$ generation could be generated requiring a specific set of cathode and air or $O_2$ bubbling. Then, when iron is added, the Fenton reaction takes place (Brillas et al., 2010; Ganiyu et al., 2020). This is called electro-Fenton (EF). As in photo-Fenton, the $Fe^{2+}$ consumed during the reaction can be regenerated by a UV light source such as sunlight, and the process is then known as solar photoelectro-Fenton (SPEF) (Moreira et al., 2017). The principles of this treatment make highly saline effluents very suitable for electrochemical systems because a high concentration of ions in the aqueous solution facilitates the flow of electrons from the anode to the cathode, by lowering ohmic resistance. Therefore, energy consumption required for the elimination of MCs may be lower than in other water matrices. The issue of efficient $H_2O_2$ dosage, during the photo-Fenton process, can also be overcome this way due to the onsite generation of this reagent on the cell cathode, during EF by reducing $O_2$ (Martínez-Huitle and Brillas, 2009).

The main objective and novelty of this study was to generate ready-to-use revalorized irrigation water for fertilization from urban wastewater treatment plant (UWWTP) effluents, based on controlled retention of salts and MCs using NF membranes at several different pH, producing a permeate free of MC, with lower conductivity and rich in $NH_4^+$. Retentates generated by NF at different concentration factors (CF) were treated by a set of novel AOPs focusing on the successful integration with NF towards an effective, cost efficient and an environmental friendly reclamation of urban wastewater.

The target was 80% MC elimination, following the Swiss regulation on MCs in UWWTP effluents (elimination of MC to 80% in all Swiss UWWTP), which is the first legislation focusing on MCs elimination (Federal Office for the Environment FOEN Water Division, 2019). First approach experiments were performed under simulated UWWTP effluents. MC commonly found in these effluents were tested in synthetic aqueous solutions that simulate the UWWTP effluents at an initial concentration of 100 μg/L each. MCs elimination by solar photo-Fenton was compared with different electrooxidation (EO) processes as anodic oxidation (AO), solar-assisted anodic oxidation (SAAO), EF and SPEF at circumneutral and alkaline pH, as retentates from NF are good candidates for EO processes due to their high salt content. Phytotoxicity and acute toxicity tests were performed on the permeate, as first approach to assess the potentially safe reuse of treated wastewater for crop irrigation.

## 2. Materials and methods

### 2.1. Reagents and chemicals

The water matrix was natural water (Tabernas, Spain; see Table SI 1 for composition). Salts were purchased from Honeywell-Fluka (NaCl), Labbox Labware S.L ($(NH_4)_2SO_4$) and Sigma-Aldrich ($Fe_2(SO_4)_3{\cdot}xH_2O$ for Fe(III)), as were the HPLC-grade solvents for MC monitoring. Selected MCs were from Fluka (Caffeine(CAF)) and Sigma-Aldrich (Imidacloprid (IMI), Thiacloprid (THI), Carbamazepine (CAR) and Diclofenac (DIC)). The reagents ($H_2O_2$ (35% w/v) and Sodium persulfate ($Na_2S_2O_8$)) were also purchased from Sigma Aldrich. $H_2SO_4$ (95–97%) and NaOH were purchased from J.T. Baker. Table SI 2 shows the molecular structure of the five selected MCs.

### 2.2. Analytical determinations

MC concentrations, dissolved organic carbon (DOC), carbonates, $H_2O_2$, persulfate and iron were determined according to the analytical methods specified in Table SI 3. Quantification limit (LOQ, 5 μg/L), and maximum absorption wavelength of selected MCs evaluated by ultra-performance liquid chromatography can be found in Table SI 4. A TOC (total organic carbon) analyzer was used to measure dissolved organic carbon and inorganic carbon. $H_2O_2$ was determined using Titanium (IV) oxysulfate following DIN 38402H15. Iron determination was performed according to ISO 6332.

The ionic composition of the samples was analyzed by ionic chromatography with a Metrohm 850 Professional IC after dilution (1:20, 1:40 and 1:100, v/v), and filtration through a 0.45-μm nylon filter. A Metrosep A Supp 7150/40 column was used for anion determination, thermoregulated at 45 °C with 3.6 mM of sodium carbonate eluent at 0.7 mL/min. A Metrosep C6 150/4.0 column was used for cation determination with 1.7 mM dipicolinic acid eluent solution at 1.2 mL/min.

The concentration of free available chlorine (FAC) was determined by Hach Method 10,069 using N, N-diethyl-*p*-phenylenediamine (DPD) powder pillows and measuring the absorbance with a Thermo Scientific Evolution 220 UV–Visible spectrophotometer at 530 nm.

### 2.3. Experimental setup

#### 2.3.1. Nanofiltration membrane pilot plant

The NF pilot plant is comprised of a 400-L feed tank with a recirculation pump, which continuously mixes the concentrate stream with the tank volume. The MC concentration increased as the volume was reduced by permeate discharge. The NF membrane, a DOW FILMTEC™ NF90–2540, spiral-wound polyamide thin-film composite membrane, works by crossflow filtration. The NF membrane has a total surface area of 2.6 $m^2$ and is operable from pH 2 to 11. In this study, the maximum system pressure was set at 10 bar. For further details, see (Deemter et al., 2021).

#### 2.3.2. Experimental procedure

A stock solution of the MC mixture containing CAF, IMI, THI, CAR and DIC was prepared in methanol. The resulting concentration was 2.5 g/L of each compound, which ensured high solubility and low DOC when diluted in water to μg/L range. The desired matrix was prepared in the feed tank (400 L) to a final concentration of 5.0 g/L of NaCl, 500.0 mg/L $NH_4^+$ and 100.0 μg/L of each MC. The system was operated at 10 bar. The main intention, being a first approach study, was to use a simple and reliable analytical method (conventional liquid chromatography) targeting several MCs, since there can be hundreds of those found in actual UWWTP effluents. Therefore, we selected five MCs with easy separation and good detection by UPLC -DAD. Initial concentration was selected low enough but affordable by UPLC-DAD (LOQ, 5 μg / L).

First, the NF pilot plant was operated until 150 L of permeate were collected. This was then stored and designated as P1. The NF process continued until another 50 L of permeate had been accumulated, and this was labelled as P2. The resulting concentrate volume ($V_C$) of about 200 L at CF = 2 was labelled as C1. Another batch was generated by running 400 L in the feed tank but disregarding the first 200 L of permeate. The NF process continued with the remaining 200 L, then another 100 L of permeate was collected and stored, and labelled as P3. The resulting $V_C$ of about 100 L was labelled C2 (CF = 4). Each effluent generated was stored in a separate vessel and kept refrigerated till further use. Average MC concentrations and main physicochemical parameters of each sample are shown in Table 1. There was a significant increase in MC concentration in permeate as NF proceeded (comparing P1, P2 and P3).

**Table 1**
Average MC concentrations [μg/L] and main physicochemical parameters of each effluent. P1, P2, P3, C1 and C2 were defined in the text.

| | P1 | P2 | P3 | C1 (CF = 2, $V_C$ = 200 L) | C2 (CF = 4, $V_C$ = 100 L) |
|---|---|---|---|---|---|
| CAF | 5 | 15 | 35 | 150 | 280 |
| IMI | 10 | 25 | 55 | 135 | 210 |
| THI | 15 | 35 | 60 | 130 | 170 |
| CAR | 5 | 5 | 10 | 150 | 300 |
| DIC | 5 | 5 | 5 | 145 | 255 |
| pH | 10 | 10 | 10 | 9 | 9 |
| $NH_4^+$ [mg/L] | 140 | 215 | 315 | 705 | 835 |
| $HCO_3^-/CO_3^{2+}$ [mg/L] | 25 | 35 | 75 | 300 | 450 |
| DOC [mg/L] | 10 | 10 | 10 | 20 | 25 |
| Conductivity [μS/cm] | 1200 | 3000 | 7750 | 22,000 | 32,000 |

#### 2.3.3. Solar photo-Fenton treatment

Solar photo-Fenton experiments were performed in a solar simulator (Atlas-SunTest XLS + ) with a daylight filter, and a xenon lamp on the chamber ceiling, programed for 365 W/$m^2$ (300–800 nm) total radiation and 30 W/$m^2$ UV radiation (300–400 nm) at a controlled temperature of 25 °C. A magnetically stirred 1-L cylindrical container (18.5 cm diameter and 4.0 cm deep) was placed in the center of the solar simulator platform. Further solar photo-Fenton experiments were scaled up to an 80-L CPC photoreactor tilted 37° (Tabernas, Spain). The 4-$m^2$ CPC irradiated surface is made up of 50-mm outer diameter borosilicate glass tubes. The global UV radiation was measured at one-minute intervals using a Kipp & Zonen CUV 5 pyranometer (280–400 nm), at a sensitivity of 301 μV/W*$m^2$ and tilted at the same angle as the CPC.

The accumulated UV solar energy needed for kinetic calculations is given by Eq. (1) (Malato et al., 2003).

$$Q_{UV,n} = Q_{UVn-1} + (t_n - t_{n-1}) * \overline{UV}_{G,n} * A_i/V_t \quad (1)$$

where $Q_{UV,n}$ [kJ/L] is the accumulated UV energy per unit of volume, $Q_{UVn-1}$ [W/$m^2$] is the average solar ultraviolet radiation 280–400 [nm] measured over a period of time, $t_n$ and $t_{n-1}$, and $n$ is the number of samples, $A_i$ is the irradiated reactor surface and $V_t$ is the total volume treated.

For the photo-Fenton experiments at circumneutral pH, bicarbonates (known $HO^{\bullet}$ radical scavengers) were removed by air stripping after addition of $H_2SO_4$, lowering $HCO_3^-$ to around 75 mg/L (final pH at 6.5–7.9). The $Fe^{3+}$:EDDS ratio ($Fe_2(SO_4)_3.7H_2O$ previously dissolved in demineralized water at pH 3, followed by EDDS addition) was 1:1 for all the experiments and initial $H_2O_2$ concentration was 1.50 mM. Operational conditions were selected according to previous process optimisation (Deemter et al., 2021). A summary of the experiments can be found in Table SI 4.

#### 2.3.4. Solar photoelectro-Fenton treatment

The electrooxidation pilot plant consists of commercial Electro MP-Cell plate-and-frame cells (ElectroCell A/S, Denmark). Each cell contained an anode of BDD thin film deposited on a Nb mesh (Nb-BDD) and a carbon-polytetrafluoroethylene GDE as the cathode, both with 100 $cm^2$ effective area connected to a 100-L feed tank and a 2 $m^2$ solar CPC photoreactor (23 L total irradiated volume). A constant current density (j) of 74

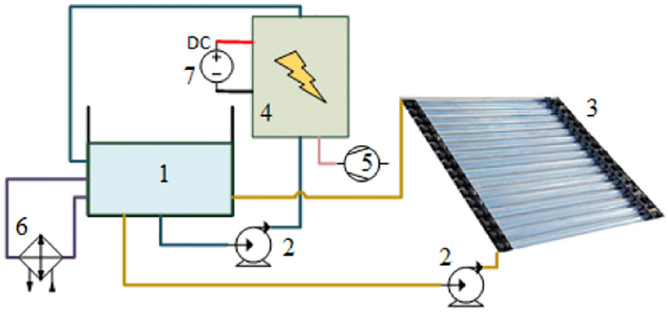


**Fig. 1.** Schematic view of the electrooxidation pilot plant and main components: 1. Tank, 2. Centrifugal pumps, 3. CPC photoreactor, 4. ElectroCell with BDD anode and carbon-PTFE (gas diffusion electrode) cathode, 5. Air compressor, 6. Heat exchanger and 7. Power supply.

$mA/cm^2$ was maintained as optimized by (Salmerón et al., 2019). The electrooxidation current density and other electrooxidation operational parameters were maintained as optimized by (Salmerón et al., 2021). The air pressure to the electrochemical cell was kept at 0.7 bar and air flow rate at 10 L/min. Treated water pressure was 0.5 bar and the flow rate 4 L/min. The air pressure and flow rate to the cell is essential to prevent water flow back into the air circuit. The experimental volume of the electrochemical system was 30 L and when combined with the CPC photoreactor, the total volume was 75 L. The setup includes an automatic cooling system which keeps the temperature at 25 °C to 30 °C (Fig. 1).

*2.3.5. Toxicity tests*

Toxicity tests were performed with commercial kits from MicroBioTests Inc. (Belgium). The PHYTOTOXKIT for Liquid Samples was applied to determine phytotoxicity according to ISO Standard 18,763, which assesses the direct effects of chemicals on seed germination and early growth of plants. Moreover, their effects were also evaluated in *Daphnia magna* by recording immobilization (acute 24 and 48 h, and chronic toxicity 72 h) with the DAPHTOXKIT F kit, with a dilution row of 100, 50, 25 and 12.5%.

## 3. Results and discussion

*3.1. Ammonium recovery by nanofiltration*

Permeation of $NH_4^+$ through commercial NF membranes was studied in a demineralized water matrix. Fig. 2 shows that $NH_4^+$ permeation was minimum at pH 4 and pH 7. At pH 9, there was substantially more permeation from a starting feed tank concentration of 250 mg/L, and higher with 500 mg/L, increasing as CF increased to CF = 4 as pH affects the speciation

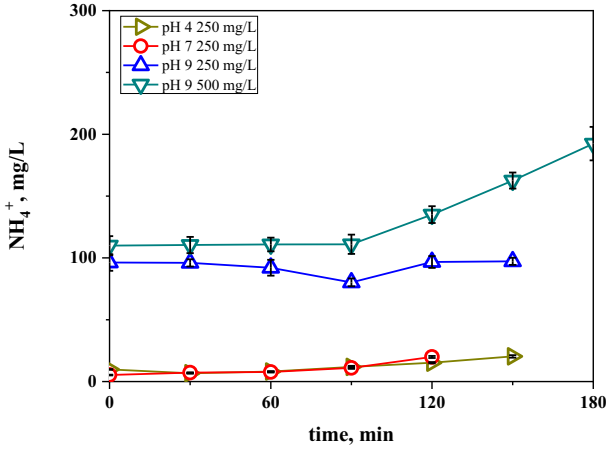


**Fig. 2.** $NH_4^+$ concentrations in mg/L in the permeate stream at different pH and feed tank concentrations. Each experiment was performed until CF = 4.

of the ammonia (at high pH ammonia molecules dominate, whereas at acidic to neutral pH ammonium ions prevail). This means that the non-charge ammonia was rejected at lower pH in comparison to the charged ammonium ions. The increased permeation with time, and consequently CF, was due to the effect of concentration polarization.

The final concentration of $NH_4^+$ in the permeate stream, that can be used as revalorized irrigation water, strongly depends on a variety of factors, such as crop, soil pH, soil consistency and type and availability and/or preference for another typical plant nitrogen source, such as $NO_3^-$. A possible negative side effect of $NH_4^+$ is that when the plant absorbs the $NH_4^+$, $H^+$ is released, acidifying the soil. Sometimes, $NH_4^+$ fertilization is even related to toxicity, making its status contradictory. NF permeates have a high pH (Table 1) and soil types in (semi-)arid areas are usually alkaline, the minor effects of soil acidification and related toxicity must be weighed against the advantages of this renewable and sustainable source of nitrogen in irrigation water for a wide variety of crops [(Britto and Kronzucker, 2002; Conklin, 2005; Hülsmann, 2018).]

To find out whether the selected MCs at a concentration of 100 μg/L each influence $NH_4^+$ permeation, experiments were performed at pH 9 and 500 mg/L $NH_4^+$. $NH_4^+$ permeation obtained was similar to Fig. 2. $NH_4^+$ permeation was also similar when the same experiments were done with water conductivity increased by adding 5 g/L NaCl. Therefore, neither the MCs in the wastewater nor water conductivity (see Table 1) influenced the permeation of $NH_4^+$. Furthermore, $NH_4^+$ recovery was highest at CF = 4, though MC permeation was also higher at that CF. Therefore, if the permeate is to be used directly as revalorized irrigation water, then CF 2, where the concentration of recovered $NH_4^+$ is high and MC permeation is low, is to be preferred.

*3.2. Solar photo-Fenton treatment of NF concentrate stream at lab and pilot scale*

Experimental parameters for MC elimination in NF concentrate by solar photo-Fenton were based on previous results with similar saline NF concentrates, ensuring minimal consumables concentration, and thereby, reducing environmental and economic impacts, while keeping elimination efficiency high (Deemter et al., 2021). Therefore, sample C2 (CF = 4) was treated by photo-Fenton in the solar lab-scale simulator using 0.10 mM Fe(III):EDDS; [1:1] and 1.50 mM $H_2O_2$ at pH 9.

High concentrations of bicarbonates from natural water (450 mg/L) were observed at pH 9, making reaction rates very slow (data not shown). Neither did the use of 1.50 mM persulfate as an oxidizing agent provide satisfactory results. Carbonates are well-known ($HO^•$) scavengers and obstruct solar photo-Fenton performance as reported elsewhere (Lado Ribeiro et al., 2019). Therefore, further experiments were performed at circumneutral pH (between 6.5 and 7.9) after addition of $H_2SO_4$ and air stripping to lower $HCO_3^-$ to <75 mg/L.

Fig. 3 shows the elimination of CAR and DIC to LOQ (5 μg/L) in 15 and 10 min, respectively. CAF, IMI and THI were more recalcitrant, reaching only 82, 54 and 55%, respectively in 15 min, with almost no degradation from 15 to 30 min, because of the low concentration of iron remaining in solution due to the decomposition of the Fe(III):EDDS complex (Gonçalves et al., 2020; Soriano-Molina et al., 2018). In fact, iron precipitation started immediately, decreasing sharply at 5 to 10 min, and was completely precipitated after 20 min. $H_2O_2$ consumption at the end of the experiment was 0.95 mM with higher consumption during the first 5 min. Blank experiments (photolysis) of CAF, IMI, THI, CAR and DIC did not reveal any substantial degradation after 30 min of illumination.

Using persulfate as an oxidizing agent at circumneutral pH, MC elimination was lower. LOQ (5 μg/L) of CAR and DIC was achieved at <5 min and CAF at <15 min. IMI and THI were more persistent, and only 24% and 20%, respectively, were eliminated. Iron concentration decreased gradually from the beginning of the treatment until only 10% was remaining after 30 min. Persulfate consumption was 0.87 mM during the first 5 min of treatment. Sulfate radicals usually show slower reaction rates than $HO^•$, which strongly depends on target MCs, starting iron, and EDDS concentration, as reported previously (Cabrera-Reina et al., 2020; Solís et al., 2020).

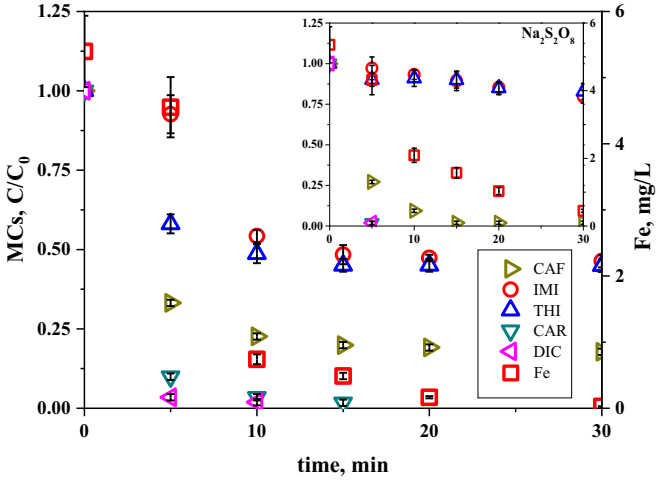


**Fig. 3.** MC concentrations and dissolved iron evolution (open red square symbol) during photo-Fenton treatment of C2 with Fe 0.10 mM, EDDS 0.10 mM and both $H_2O_2$ and persulfate (inserted figure) at 1.5 mM in the solar simulator at circumneutral pH.

Fig. 4 shows solar photo-Fenton treatment of C2 at pilot scale in an 80-L CPC photoreactor, as a function of solar accumulated UV energy (Eq. (1)) collected in the photoreactor after 30 min. Only DIC was eliminated to LOQ (5 μg/L) at <30 min, and 93% CAR was degraded, whereas CAF, IMI and THI, as in the solar simulator, were more recalcitrant, reaching only 70, 49 and 39% elimination at 30 min, respectively. Total MC elimination was 76% with accumulated UV energy of only 1.6 kJ/L. Over 90% of the Fe(III):EDDS complex was degraded in the first 30 min, confirming the inefficient elimination of MCs at circumneutral pH after complex degradation. $H_2O_2$ consumption at the end of the experiment was 0.83 mM.

### 3.3. Electrooxidation treatments

Electrooxidation experiments were performed in the SPEF pilot plant with the experimental parameters described in Section 2.3.4. Since the aim of NF is to lower the economic impact by reducing the volume of contaminated streams, the first electrooxidation treatments were performed on C2 (CF = 4), the most concentrated stream, for better comparison with the following electrooxidation treatments. Higher ionic, carbonate and MC concentrations showed increased radical scavenger effects, as mentioned above.

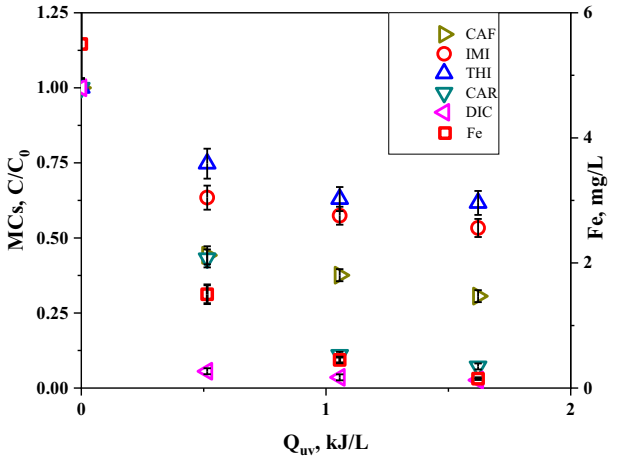


**Fig. 4.** MC concentrations and dissolved iron during solar photo-Fenton treatment of C2 at circumneutral pH in the pilot plant.

Fig. 5 shows the results with C1 with its natural carbonate concentration and applying AO, SAAO, EF and SPEF oxidation treatments. With AO, MC elimination to LOQ (5 μg/L) was only attained for CAF, THI, CAR and DIC at <150, <180, <45 and < 150 min, respectively. IMI was persistent with only 67% degradation, but the treatment still eliminated 88% of the total MCs. In SAAO, only CAR and DIC were degraded to the LOQ (5 μg/L) at 180 and 45 min, respectively, and CAF was degraded by 84%. The more persistent IMI and THI were degraded 44% and 57%, for a total MC removal of 78% at the end of the treatment. Finally, when SPEF was applied, CAR and DIC were eliminated to LOQ (5 μg/L) at <180 and < 45 min, respectively. CAF, IMI and THI were again more persistent, and were degraded only 82%, 44% and 78%, respectively. Total MC elimination was 80%.

The 80% MC removal target in concentrate C1 was not achieved by EF after 240 min of treatment. Moreover, more consumables were needed than in AO, such as EDDS, which drastically increases DOC and competes with the MCs for the radicals. Furthermore, it consumed over 50% more electricity and produced more free available chlorine (FAC) than AO. Chlorate production was reduced by 15%. Therefore, it was discarded as a suitable treatment for this kind of water as previously reported by (Salmerón et al., 2021).

The target of 80% total MC degradation was reached after 120 min with the AO treatment. Total electricity consumption was 6.1 kWh/m$^3$ for an experimental volume of 30 L. The final concentration of FAC produced was 3.4 mg/L and chlorate production started to be recorded at 10 min with 20.4 mg/L, increasing linearly to 70.0 mg/L after 240 min.

Both FAC and chlorate are by-products of the EO processes. The by-products are formed from the high concentrations of free dissolved ions in the matrix, in this case chloride. Active chlorine can be generated from free dissolved chloride ions and is widely used in wastewater treatment. Active chlorine species (ACS) are formed from the adsorbed free dissolved ions on the anode surface, resulting in the radical or other oxidizing species of the related ion. Indirect ACS are formed when the oxidizing species, previously generated, acts as an intermediate in the reaction with the MCs in the bulk of the matrix furthest from the anode (Panizza and Cerisola, 2009). ACS, which promotes MC degradation, in what is also called electrochlorination, has the advantage over conventional chlorine treatments of improved performance and absence of potentially dangerous Cl transport and storage (Martínez-Huitle and Brillas, 2009; Mostafa et al., 2018). Chlorates are formed by the reaction of ACS with $^{\bullet}$OH when a BDD anode is used (Sánchez-Carretero et al., 2011). The original C1 (CF = 2) ionic concentrations are summarized in Table SI 6.

With SAAO, the MC degradation did not quite reach the target of 80%, with only 78% after 240 min, and consumed a total of 3.8 kWh/m$^3$

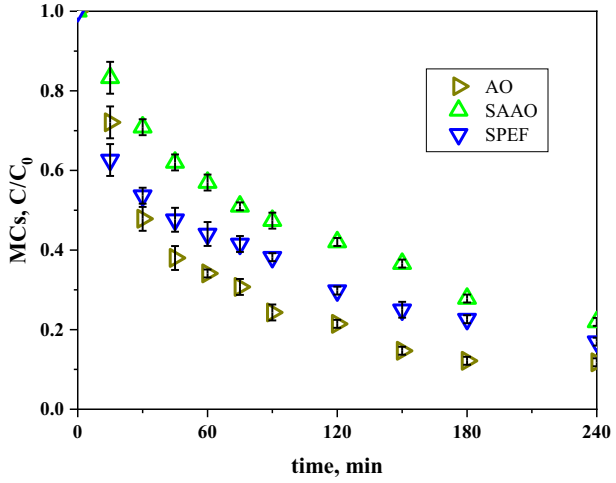


**Fig. 5.** MC concentrations during AO, SAAO and SPEF treatment at natural pH of C1 (CF = 2).

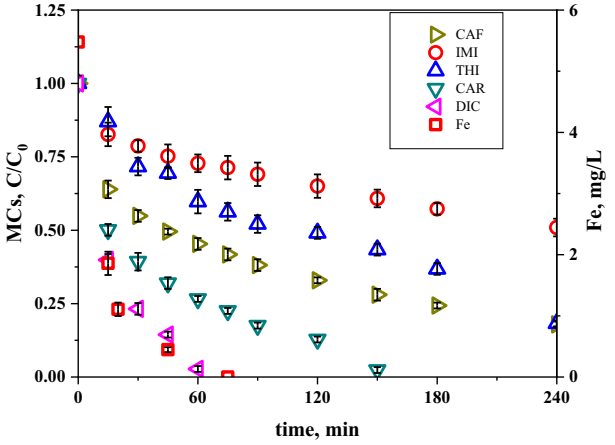


**Fig. 6.** MC concentrations during pilot-scale SPEF treatment of concentrate C1 (CF = 2) at natural pH and with low carbonate concentration.

electricity, 62% lower than AO alone, and also requiring $Q_{UV}$ of 13.3 kJ/L for an experimental volume of 75 L. FAC concentration was 4.2 mg/L, along with 33.3 mg/L of chlorate, which is an increase of 23% and 52% respectively from AO.

Finally, 80% degradation was reached at <240 min with the SPEF treatment, which required total electricity consumption of 4.2 kWh/$m^3$ and $Q_{UV}$ of 14.2 kJ/L for an experimental volume of 75 L; 11% and 7% higher than SAAO, respectively. MC degradation enhancement by addition of the Fe:EDDS was minimal due to the increase in DOC when EDDS is added. FAC concentration was only 2.1 mg/L at the end of the experiment. Chlorate production was low, with a final concentration of 16.4 mg/L, 50% lower than SAAO, due to the reaction between $H_2O_2$ and ACS.

Initial reaction rate ($r_0$) was calculated to compare the different EO processes using mass of MC instead of concentration due to the difference in experimental volume, as shown in Eq. (2).

$$r_0 = \frac{(m_{n+1} - m_n)}{(t_{n+1} - t_n)} \quad (2)$$

where $m_n$ is the cumulative MC mass at designated time in mg, calculated for the MC concentration and the volume of water treated, 30 L for AO and 75 L for SAAO and SPEF, and $t_n$ is the time interval in minutes yielding $r_0$ in mg/min. For AO, SAAO and SPEF $r_0 = -0.337$; $-0.0696$ and $-1.305$ mg/min, respectively.

Fig. 6 shows the SPEF treatment results for C1, but with a lower concentration of bicarbonates (76.3 mg/L). The purpose was to find out whether a high concentration of carbonates would be as detrimental as in the photo-Fenton process (Deemter et al., 2021). Only CAR and DIC were eliminated to LOQ (5 μg/L) at 150 and 60 min, respectively. CAF and THI were both degraded 82%, while IMI was the most persistent with 49% degradation. Total MC elimination was still 82%, demonstrating that the influence of carbonates was negligible in the SPEF treatment, and that the oxidation of MCs occurred mainly through oxidants other than HO•. Therefore, analysis of the chlorinated byproducts would be critical for the overall assessment of the system and before the design of the most appropriate treatment.

At the low carbonate concentration, SPEF treatment reached the target degradation of 80% after <220 min with a total electricity consumption of 4.3 kWh/$m^3$ and a $Q_{UV}$ of 11.6 kJ/L. FAC production was the highest of all treatments, and over double the experiment with the high carbonate concentration, ending with a concentration of 5.7 mg/L. The final chlorate concentration was 18.2 mg/L, again, similar to treatment with the high carbonate concentration. SPEF at the low carbonate concentration had a $r_0 = -1.155$ mg/min, 11% lower than with the high carbonate concentration.

### 3.4. Toxicity tests

As one of the main objectives of this study was recovery and reuse of $NH_4^+$ from the NF permeate stream obtained by pre-concentration of a UWWTP effluent for crop irrigation, phytotoxicity tests were done at two different permeate concentrations at CF = 2 and 4, to evaluate its effects on seed germination, and root and shoot growth. Permeates were tested at pH 7. The CF = 2 and 4 permeates slightly affected *Sorghum saccharatum* reducing germination 10%. CF = 2 also caused 10% less germination in *Sinapis alba*.

In *Sorghum saccharatum*, the CF = 2 permeate promoted 45% more root development than the reference with demineralized water. *S. alba* root development was 17% better with CF = 2. Root development of *Lepidium sativum* was severely affected, showing a 27% and 46% reduction with CF = 2 and 4, respectively.

*Sorghum saccharatum* shoot length was reduced 40% with CF = 4. CF = 2, however, increased it 13%. Shoot growth of *Sinapis alba* was reduced 9% and 39% with CF = 2 and 4, respectively. Finally, *Lepidium sativum* shoot growth was promoted by CF = 2, increasing it by 11%, while CF = 4 decreased it by 17%.

This means that direct application of permeate at CF = 2 was adequate for crop irrigation, in view of both root and shoot growth results. It was not the case for CF = 4, attributed to the higher concentration of MCs contained in permeate, as well as the high salt content (Fig. 7).

The DAPHTOXKIT F test was also applied to determine acute toxicity at 24 and 48 h and chronic toxicity at 72 h. Immobilization of *Daphnia magna* was assessed and compared to a freshwater control. Results are shown in Fig. 8. After 24 h, there was no immobilization at the 12.5, 25 and 50% CF = 2 dilutions. At 100% of CF = 2, only one of the organisms showed some movement. Results were similar in CF = 4, except for the 100% sample, where all organisms were immobilized. After 48 h, samples containing 12.5, 25 and 50% dilutions in CF = 2 showed 0, 2 and 3 out of 5 immobilized organisms, respectively. At 100%, all organisms were

**Fig. 7.** Photos of phytotoxicity test, from left to right, *Sinapis alba*, *Sorghum saccharatum* and *Lepidium sativum*. All three species showed full germination.

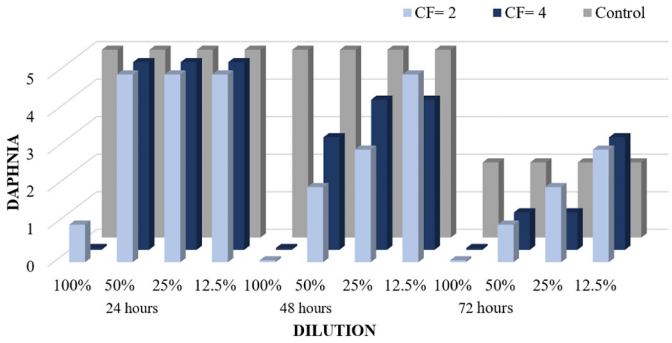


**Fig. 8.** Acute (24 and 48 h) and chronic (72 h) toxicity tests with *Daphnia magna* organisms at different dilutions in freshwater. CF = 2 (front) and CF = 4 (middle) permeates and freshwater control (back).

immobilized. In CF = 4, results were similar. Finally, after 72 h, 3 out of 5 organisms in the control sample were immobilized. CF = 2 showed 2, 3 and 4 immobilized organisms in 12.5, 25 and 50% dilutions, whereas in CF = 4 results were similar. Therefore, both permeate volumes should be diluted at least 50%, to prevent osmotic stress and acute toxicity. At a 25% dilution, only CF = 2 showed chronic toxicity results similar to freshwater.

## 4. Conclusions

$NH_4^+$ can effectively be recovered from wastewater using NF at pH 9. NF treatment to a concentration factor of 2 was able to produce a ready-to-use permeate stream with recovered $NH_4^+$. However, despite NF would leads to the elimination of bacteria, in case of antibiotic resistance genes and antibiotic resistant bacteria it is not enough. Therefore, such effect must be checked before crop irrigation.

Persulfate was a less efficient oxidizing agent than $H_2O_2$ by solar photo-Fenton. As dissolved iron quickly disappeared at circumneutral pH, it would only be of interest for rapid degradation of contaminants at less than 1 mg/L in NF retentate. Other alternative tertiary treatments, such as electrooxidation processes, are a promising alternative when a high concentration of MC requires longer treatment times. Analysis of the chlorinated byproducts would be critical for the overall assessment and before the design of the most appropriate treatment.

Solar-assisted anodic oxidation significantly reduced the electricity consumption necessary for degradation and residual FAC and chlorate concentrations were lower than with anodic oxidation. Solar photoelectron-Fenton showed results similar to solar assisted anodic oxidation, but required more consumables. Electro-Fenton was the least efficient of the electro oxidation processes tested.

Phytotoxicity results showed that irrigation with the permeates slightly affected germination. Acute and chronic *Daphnia magna* toxicity studies demonstrated that the permeate volumes should be diluted at least 50% before direct reuse for crop irrigation.

## CRediT authorship contribution statement

**Dennis Deemter:** Conceptualization, Formal analysis, Methodology, Investigation, Writing – original draft. **Irene Salmerón:** Conceptualization, Formal analysis, Methodology, Investigation, Writing – original draft. **Isabel Oller:** Validation, Writing – review & editing, Supervision, Funding acquisition, Project administration. **Ana M. Amat:** Writing – review & editing. **Sixto Malato:** Supervision, Writing – review & editing, Funding acquisition, Project administration.

## Declaration of competing interest

The authors declare that they have no known competing financial interests or personal relationships that could have appeared to influence the work reported in this paper.

## Acknowledgement

This study is part of a project funded by the European Union's Horizon 2020 research and innovation program under Marie Skłodowska-Curie Grant Agreement No 765860. The authors also wish to thank the Spanish Ministry of Science, Innovation and Universities (MCIU), AEI and FEDER for funding under the NAVIA Project (ID2019-110441RB-C32).

## Appendix A. Supplementary data

Supplementary data to this article can be found online at https://doi.org/10.1016/j.scitotenv.2022.153693.

## References

Balogun, H.A., Sulaiman, R., Marzouk, S.S., Giwa, A., Hasan, S.W., 2019. 3D printing and surface imprinting technologies for water treatment: a review. J. Water Process Eng. 31, 100786. https://doi.org/10.1016/j.jwpe.2019.100786.

Brillas, E., Sirés, I., Cabot, P.L., 2010. Use of both anode and cathode reactions in wastewater treatment. In: Comninellis, C., Chen, G. (Eds.), Electrochem. Environ. Springer New York, New York, NY, pp. 515–552 https://doi.org/10.1007/978-0-387-68318-8_19.

Britto, D.T., Kronzucker, H.J., 2002. NH4+ toxicity in higher plants: a critical review. J. Plant Physiol. 159, 567–584. https://doi.org/10.1078/0176-1617-0774.

Cabrera-Reina, A., Miralles-Cuevas, S., Oller, I., Sánchez-Pérez, J.A., Malato, S., 2020. Modeling persulfate activation by iron and heat for the removal of contaminants of emerging concern using carbamazepine as model pollutant. Chem. Eng. J. 389, 124445. https://doi.org/10.1016/j.cej.2020.124445.

Castro-Muñoz, R., Fíla, V., 2018. Membrane-based technologies as an emerging tool for separating high-added-value compounds from natural products. Trends Food Sci. Technol. 82, 8–20. https://doi.org/10.1016/j.tifs.2018.09.017.

Chen, C., Dong, T., Han, M., Yao, J., Han, L., 2020. Ammonium recovery from wastewater by Donnan Dialysis: a feasibility study. J. Clean. Prod. 265, 121838. https://doi.org/10.1016/j.jclepro.2020.121838.

Comer, B.M., Fuentes, P., Dimkpa, C.O., Liu, Y.H., Fernandez, C.A., Arora, P., Realff, M., Singh, U., Hatzell, M.C., Medford, A.J., 2019. Prospects and challenges for solar fertilizers. Joule. 3, 1578–1605. https://doi.org/10.1016/j.joule.2019.05.001.

Conklin A.R., Introduction to Soil Chemistry: Analysis and Instrumentation, 2005. doi: https://doi.org/10.1002/0471728225.

Deemter, D., Oller, I., Amat, A.M., Malato, S., 2021. Effect of salinity on preconcentration of contaminants of emerging concern by nanofiltration: application of solar photo-Fenton as a tertiary treatment. Sci. Total Environ. 756 143593 https://doi.org/10.1016/j.scitotenv.2020.143593.

Farré, M., 2020. Remote and in-situ devices for the assessment of marine contaminants of emerging concern and plastic debris detection. Curr. Opin. Environ. Sci. Heal. https://doi.org/10.1016/j.coesh.2020.10.002.

Federal Office for the Environment FOEN Water Division, Reporting for Switzerland under the Protocol on Water and Health, 2019.

Fernández-Delgado, M., del Amo-Mateos, E., Lucas, S., García-Cubero, M.T., Coca, M., 2020. Recovery of organic carbon from municipal mixed waste compost for the production of fertilizers. J. Clean. Prod. 265. https://doi.org/10.1016/j.jclepro.2020.121805.

Ganiyu, S.O., Martínez-Huitle, C.A., Rodrigo, M.A., 2020. Renewable energies driven electrochemical wastewater/soil decontamination technologies: a critical review of fundamental concepts and applications. Appl. Catal. B Environ. 270 118857 https://doi.org/10.1016/j.apcatb.2020.118857.

Gerardo, M.L., Aljohani, N.H.M., Oatley-Radcliffe, D.L., Lovitt, R.W., 2015. Moving towards sustainable resources: recovery and fractionation of nutrients from dairy manure digestate using membranes. Water Res. 80, 80–89. https://doi.org/10.1016/j.watres.2015.05.016.

Gonçalves, B.R., Guimarães, R.O., Batista, L.L., Ueira-Vieira, C., Starling, M.C.V.M., Trovó, A.G., 2020. Reducing toxicity and antimicrobial activity of a pesticide mixture via photo-Fenton in different aqueous matrices using iron complexes. Sci. Total Environ. 740, 140152. https://doi.org/10.1016/j.scitotenv.2020.140152.

Hargreaves, J.S.J., Chung, Y.M., Ahn, W.S., Hisatomi, T., Domen, K., Kung, M.C., Kung, H.H., 2020. Minimizing energy demand and environmental impact for sustainable NH3 and H2O2 production—a perspective on contributions from thermal, electro-, and photocatalysis. Appl. Catal. A Gen. 594, 117419. https://doi.org/10.1016/j.apcata.2020.117419.

Horikoshi, S., Serpone, N., 2020. Can the photocatalyst TiO2 be incorporated into a wastewater treatment method? Background and prospects. Catal. Today 340, 334–346. https://doi.org/10.1016/j.cattod.2018.10.020.

Hülsmann S., Managing water, soil and waste resources to achieve sustainable development goals, 2018. doi: https://doi.org/10.1007/978-3-319-75163-4.

Lado Ribeiro, A.R., Moreira, N.F.F., Li, Puma G., Silva, A.M.T., 2019. Impact of water matrix on the removal of micropollutants by advanced oxidation technologies. Chem. Eng. J. 363, 155–173. https://doi.org/10.1016/j.cej.2019.01.080.

López-Rayo, S., Sanchis-Pérez, I., Ferreira, C.M.H., Lucena, J.J., 2019. [S,S]-EDDS/Fe: a new chelate for the environmentally sustainable correction of iron chlorosis in calcareous soil. Sci. Total Environ. 647, 1508–1517. https://doi.org/10.1016/j.scitotenv.2018.08.021.

Malato, S., Blanco, J., Campos, A., Cáceres, J., Guillard, C., Herrmann, J.M., Fernández-Alba, A.R., 2003. Effect of operating parameters on the testing of new industrial titania

catalysts at solar pilot plant scale. Appl. Catal. B Environ. 42, 349–357. https://doi.org/10.1016/S0926-3373(02)00270-9.
Malato, S., Fernández-Ibáñez, P., Maldonado, M.I., Blanco, J., Gernjak, W., 2009. Decontamination and disinfection of water by solar photocatalysis: recent overview and trends. Catal. Today 147, 1–59. https://doi.org/10.1016/j.cattod.2009.06.018.
Martínez-Huitle, C.A., Brillas, E., 2009. Decontamination of wastewaters containing synthetic organic dyes by electrochemical methods: a general review. Appl. Catal. B Environ. 87, 105–145. https://doi.org/10.1016/j.apcatb.2008.09.017.
Mendret, J., Azais, A., Favier, T., Brosillon, S., 2019. Urban wastewater reuse using a coupling between nanofiltration and ozonation: techno-economic assessment. Chem. Eng. Res. Des. 145, 19–28. https://doi.org/10.1016/j.cherd.2019.02.034.
Miralles-Cuevas, S., Oller, I., Agüera, A., Sánchez Pérez, J.A., Malato, S., 2017. Strategies for reducing cost by using solar photo-Fenton treatment combined with nanofiltration to remove microcontaminants in real municipal effluents: toxicity and economic assessment. Chem. Eng. J. 318, 161–170. https://doi.org/10.1016/j.cej.2016.06.031.
Moreira, F.C., Boaventura, R.A.R., Brillas, E., Vilar, V.J.P., 2017. Electrochemical advanced oxidation processes: a review on their application to synthetic and real wastewaters. Appl. Catal. B Environ. 202, 217–261. https://doi.org/10.1016/j.apcatb.2016.08.037.
Mostafa, E., Reinsberg, P., Garcia-Segura, S., Baltruschat, H., 2018. Chlorine species evolution during electrochlorination on boron-doped diamond anodes: in-situ electrogeneration of Cl2, Cl2O and ClO2. Electrochim. Acta 281, 831–840. https://doi.org/10.1016/j.electacta.2018.05.099.
Nath, K., Dave, H.K., Patel, T.M., 2018. Revisiting the recent applications of nanofiltration in food processing industries: progress and prognosis. Trends Food Sci. Technol. 73, 12–24. https://doi.org/10.1016/j.tifs.2018.01.001.
Panizza, M., Cerisola, G., 2009. Direct and mediated anodic oxidation of organic pollutants. Chem. Rev. 109, 6541–6569. https://doi.org/10.1021/cr9001319.
Patel, A., Mungray, A.A., Mungray, A.K., 2020. Technologies for the recovery of nutrients, water and energy from human urine: a review. Chemosphere. 259, 127372. https://doi.org/10.1016/j.chemosphere.2020.127372.
Sakar, H., Celik, I., Balcik-Canbolat, C., Keskinler, B., Karagunduz, A., 2019. Ammonium removal and recovery from real digestate wastewater by a modified operational method of membrane capacitive deionization unit. J. Clean. Prod. 215, 1415–1423. https://doi.org/10.1016/j.jclepro.2019.01.165.
Salmerón, I., Plakas, K.V., Sirés, I., Oller, I., Maldonado, M.I., Karabelas, A.J., Malato, S., 2019. Optimization of electrocatalytic H2O2 production at pilot plant scale for solar-assisted water treatment. Appl. Catal. B Environ. 242, 327–336. https://doi.org/10.1016/j.apcatb.2018.09.045.
Salmerón, I., Rivas, G., Oller, I., Martínez-Piernas, A., Agüera, A., Malato, S., 2021. Nanofiltration retentate treatment from urban wastewater secondary effluent by solar electrochemical oxidation processes. Sep. Purif. Technol. 254, 117614. https://doi.org/10.1016/j.seppur.2020.117614.
Sánchez-Carretero, A., Sáez, C., Cañizares, P., Rodrigo, M.A., 2011. Electrochemical production of perchlorates using conductive diamond electrolyses. Chem. Eng. J. 166, 710–714. https://doi.org/10.1016/j.cej.2010.11.037.
Schäfer, A.I., Fane, A.G., 2021. Nanofiltration: Principles, Applications, and New Materials. John Wiley & Sons.
Seibert, D., Zorzo, C.F., Borba, F.H., de Souza, R.M., Quesada, H.B., Bergamasco, R., Baptista, A.T., Inticher, J.J., 2020. Occurrence, statutory guideline values and removal of contaminants of emerging concern by electrochemical advanced oxidation processes: a review. Sci. Total Environ. 748, 141527. https://doi.org/10.1016/j.scitotenv.2020.141527.
Solís, R.R., Rivas, F.J., Chávez, A.M., Dionysiou, D.D., 2020. Peroxymonosulfate/solar radiation process for the removal of aqueous microcontaminants. Kinetic modeling, influence of variables and matrix constituents. J. Hazard. Mater. 400. https://doi.org/10.1016/j.jhazmat.2020.123118.
Soriano-Molina, P., García Sánchez, J.L., Malato, S., Pérez-Estrada, L.A., Sánchez Pérez, J.A., 2018. Effect of volumetric rate of photon absorption on the kinetics of micropollutant removal by solar photo-Fenton with Fe 3+ -EDDS at neutral pH. Chem. Eng. J. 331. https://doi.org/10.1016/j.cej.2017.08.096.
Suwaileh, W., Johnson, D., Hilal, N., 2020. Membrane desalination and water re-use for agriculture: state of the art and future outlook. Desalination. 491, 114559. https://doi.org/10.1016/j.desal.2020.114559.
Taylor, A.C., Fones, G.R., Mills, G.A., 2020. Trends in the use of passive sampling for monitoring polar pesticides in water. Trends Environ. Anal. Chem. 27, e00096. https://doi.org/10.1016/j.teac.2020.e00096.
Temara, A., Bowmer, T., Rottiers, A., Robertson, S., 2006. Germination and seedling growth of the water cress Rorippa sp. exposed to the chelant [S,S]-EDDS. Chemosphere. 65, 716–720. https://doi.org/10.1016/j.chemosphere.2006.01.067.
van Gils, J., Posthuma, L., Cousins, I.T., Brack, W., Altenburger, R., Baveco, H., Focks, A., Greskowiak, J., Kühne, R., Kutsarova, S., Lindim, C., Markus, A., van de Meent, D., Munthe, J., Schueder, R., Schüürmann, G., Slobodnik, J., de Zwart, D., van Wezel, A., 2020. Computational material flow analysis for thousands of chemicals of emerging concern in European waters. J. Hazard. Mater. 397, 122655. https://doi.org/10.1016/j.jhazmat.2020.122655.
Wang, R., Lin, S., 2021. Pore model for nanofiltration: history, theoretical framework, key predictions, limitations, and prospects. J. Membr. Sci. 620, 118809. https://doi.org/10.1016/j.memsci.2020.118809.
Wang, X., Dong, W., Brigante, M., Mailhot, G., 2019. Hydroxyl and sulfate radicals activated by Fe(III)-EDDS/UV: comparison of their degradation efficiencies and influence of critical parameters. Appl. Catal. B Environ. 245, 271–278. https://doi.org/10.1016/j.apcatb.2018.12.052.
Wang, S., Li, L., Yu, S., Dong, B., Gao, N., Wang, X., 2021. A review of advances in EDCs and PhACs removal by nanofiltration: mechanisms, impact factors and the influence of organic matter. Chem. Eng. J. 406, 126722. https://doi.org/10.1016/j.cej.2020.126722.
Wei, S.P., van Rossum, F., van de Pol, G.J., Winkler, M.K.H., 2018. Recovery of phosphorus and nitrogen from human urine by struvite precipitation, air stripping and acid scrubbing: a pilot study. Chemosphere. 212, 1030–1037. https://doi.org/10.1016/j.chemosphere.2018.08.154.
Xu, R., Qin, W., Zhang, B., Wang, X., Li, T., Zhang, Y., Wen, X., 2020. Nanofiltration in pilot scale for wastewater reclamation: long-term performance and membrane biofouling characteristics. Chem. Eng. J. 395, 125087. https://doi.org/10.1016/j.cej.2020.125087.
Yusuf, A., Sodiq, A., Giwa, A., Eke, J., Pikuda, O., De Luca, G., Di Salvo, J.L., Chakraborty, S., 2020. A review of emerging trends in membrane science and technology for sustainable water treatment. J. Clean. Prod. 266, 121867. https://doi.org/10.1016/j.jclepro.2020.121867.
Zeng, X., Zou, D., Wang, A., Zhou, Y., Liu, Y., Li, Z., Liu, F., Wang, H., Zeng, Q., Xiao, Z., 2020. Remediation of cadmium-contaminated soils using Brassica napus: effect of nitrogen fertilizers. J. Environ. Manag. 255, 109885. https://doi.org/10.1016/j.jenvman.2019.109885.